Photochemistry and Photobiology, 20**, **: *–*

Photodynamic Effects of Zinc(II) Phthalocyanine-Loaded Polymeric Micelles in Human Nasopharynx KB Carcinoma Cells

María C. García Vior[1], Julieta Marino[2], Leonor P. Roguin[2], Alejandro Sosnik[3] and Josefina Awruch*[1]

[1]Departamento de Química Orgánica, Facultad de Farmacia y Bioquímica, Universidad de Buenos Aires, Buenos Aires, Argentina
[2]Instituto de Química y Fisicoquímica Biológicas (UBA-CONICET), Facultad de Farmacia y Bioquímica, Buenos Aires, Argentina
[3]BIONIMED, Departamento de Tecnología Farmacéutica, Facultad de Farmacia y Bioquímica, Buenos Aires, Argentina

Received 19 June 2012, accepted 13 August 2012, DOI: 10.1111/j.1751-1097.2012.01229.x

ABSTRACT

A major difficulty in photodynamic therapy is the poor solubility of the photosensitizer (PS) under physiological conditions which correlates with low bioavailability. PS aggregation leads to a decrease in the photodynamic efficiency and a more limited activity *in vitro* and *in vivo*. To improve the aqueous solubility and reduce the aggregation of 2,9(10),16(17),23(24)-tetrakis[(2-dimethylamino)ethylsulfanyl] phthal-ocyaninatozinc(II) (Pc9), the encapsulation into four poloxamine polymeric micelles (T304, T904, T1107 and T1307) displaying a broad spectrum of molecular weight and hydrophilic–lipophilic balance was investigated. The aqueous solubility of Pc9 was increased up to 30 times. Morphological evaluation showed the formation of Pc9-loaded spherical micelles in the nanosize range. UV/Vis and fluorescence studies indicated that Pc9 is less aggregated upon encapsulation in comparison with Pc9 in water–DMSO 2% and remained photostable. Pc9-loaded micelles generated singlet molecular oxygen in high yields. Photocytotoxicity assays using human nasopharynx KB carcinoma cells confirmed that the encapsulation of Pc9 in T1107 and T1307 increases its photocytotoxicity by 10 times in comparison with the free form in water–DMSO. In addition, Pc9 incorporated into cells was mainly localized in lysosomes.

INTRODUCTION

Cancer is one of the most devastating diseases worldwide, with an estimated 7.9 million deaths in 2007 and an expected increase to 12 million by 2030. Photodynamic therapy (PDT) is a promising clinical treatment of a variety of endoscopically accessible tumors, such as lung, bladder, gastrointestinal and gynecological neoplasms, as well as nonmelanoma skin cancer and precancerous diseases (1–7). The clinical treatment involves the administration of a photosensitizing (PS) agent, which preferentially localizes within the tumor, followed by irradiation with visible light of an appropriate wavelength of the targeted tissue. This process generates reactive oxygen species capable of reacting with lipids and proteins in cancer tissue, leading to necrosis or apoptosis and tumor ablation (8).

Phthalocyanines (Pcs) have found applications as phototoxic drugs for PDT (2,9–11). In addition to their well-known chemical stability, Pcs exhibit a high absorption coefficient (10^5 M^{-1} cm^{-1}) in the visible region of the spectrum, mainly in the phototherapeutic window (600–800 nm) and an efficient singlet oxygen production, the predominant cytotoxic agent responsible for cancer cell damage (12). It has been reported that thiol-derivatized metallophthalocyanine complexes show excellent spectroscopic and photochemical properties, such as wavelength absorption over 700 nm, higher values of molar absorption coefficients in comparison with alkyl-substituted Pcs. These features allow the use of light displaying greater skin penetration, and enhance the photocytotoxic effects due to a higher singlet oxygen photogeneration (13–15). An important aspect that needs to be considered is the strong tendency of Pcs to form aggregates. This aggregation is usually attributed to a coplanar association of rings progressing from monomer to dimer and to higher order complexes, which affect the optical properties of Pcs diminishing their photodynamic efficiency. Through the use of different nanocarriers, aggregation can sometimes be partially or completely prevented and the solubility of PS can be increased, thus allowing parenteral administration (16). As improved solubility usually correlates with higher bioavailability (17,18), several nanocarriers (*e.g.* liposomes, dendrimers, polymeric nanoparticles and nanoemulsions) are being explored to guarantee the appropriate PS solubilization and delivery (19–22). The *in vitro* PDT efficacy of silicon(IV) phthalocyanines incorporated into polymeric micelles has been established (21,23).

Polymeric micelles are nanoscopic (≤ 100 nm) structures generated by the self-assembly of amphiphilic block copolymers in water above the critical micelle concentration (CMC) (24,25). Polymeric micelles display several advantages over the standard micelles such as polysorbate 80 (Tween 80®) and polyethoxylated castor oil (Cremophor EL®). They solubilize drugs more effectively, they are safer for parenteral administration and they are more physically stable under dilution (26,27). The thermo-responsive poly(ethylene oxide)poly(propylene oxide) (PEO-PPO) block copolymers are among the most extensively investigated micelle-forming amphiphiles (24). Poloxamines (Tetronic®) are X-shaped amphiphilic block copolymers formed by four PEO-PPO blocks linked to a central ethylenediamine group, the latter conferring the amphiphile dual responsiveness to temperature and pH. Due to the

*Corresponding author email: jawruch@ffyb.uba.ar (Josefina Awruch)

unique arrangement where the hydrophobic blocks form the inner core and the hydrophilic ones the outer corona, polymeric micelles can host lipophilic drug molecules within the core and improve their aqueous solubility and stability (28,29).

The great interest to improve the photodynamic performance of 2,9(10),16(17),23(24)-tetrakis[(2–dimethylamino)ethylsulfanyl] phthalocyaninatozinc(II) (Pc9), a derivative that has shown promising photodynamic properties (14), has led us to investigate the encapsulation of Pc9 into four different poloxamine polymeric micelles of different size and hydrophilic–lipophilic balance (HLB). The spectroscopic and photophysical properties, as well as the size, the solubility and the photochemical stability were comprehensibly investigated. Finally, the photocytotoxicity of the formulated micellar Pc9 was assayed in human nasopharynx KB carcinoma cells and compared with that of the free Pc9. The uptake and the intracellular localization of the encapsulated phthalocyanine were also explored.

MATERIALS AND METHODS

Materials. Pc9 (Fig. 1) was synthesized in our laboratory as previously described (14). Poloxamines Tetronic® 304 (T304, MW 1.65 kDa), 904 (T904, MW 6.7 kDa), 1107 (T1107, MW 15 kDa) and 1307 (T1307, MW 18 kDa) were a gift from BASF. Diphenylbenzofuran (DPBF), imidazol BioUltra and Methylene Blue hydrate (MB) were obtained from Fluka (India). *N*,*N*-Diethyl-4-nitrosoaniline 97%, dimethylsulfoxide (DMSO), acetone, tetrahydrofuran (THF) and spectrophotometric grade were obtained from Sigma–Aldrich (Germany). All chemicals were of reagent grade and used without further purification. Milli-Q water was obtained from a Milli-Q system (Millipore).

Preparation of polymeric micelles. Polymeric micelles (10% wt/vol) were prepared by dissolving the required amount of copolymer in milli-Q water (pH 7–8) at 4°C followed by the equilibration of the system at 25° C, for at least 24 h before use.

Encapsulation of Pc9. A 0.5 mM solution of Pc9 in acetone (200 μL) was added dropwise to the different micellar systems (5 mL) with magnetic stirring and the samples were shaken for 48 h at 25°C. The resulting suspensions were filtered through a cellulose nitrate filter (0.45 μm) to remove insoluble Pc9 and then freeze dried (FIC-L05 freeze-dryer, Scientific Instrumental Manufacturing, Argentina). Dry specimens were redissolved in acetone to fully release the Pc9 from the micelles and the concentration of Pc9 for each sample was determined by the absorbance at 685 nm (Shimadzu UV-3101 PC spectrophotometer; Shimadzu). Concentrations were calculated by interpolating the absorbance of each sample in a calibration curve of Pc9 in acetone covering the range between 0.05 and 6.9 μg mL^{-1}, which obey the linearity of the Lambert –Beer law. Samples were diluted as required to fit the calibration curve

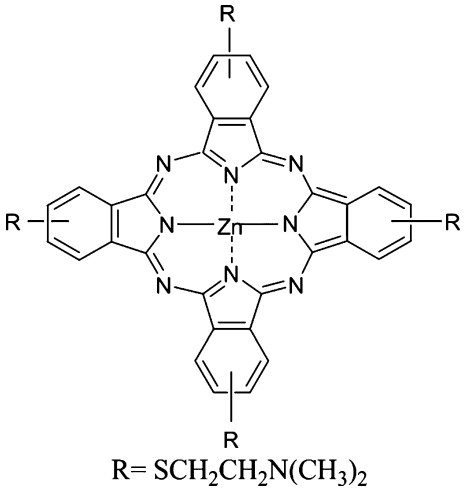

Figure 1. Chemical structure of phthalocyanine (Pc9).

range. The correlation factor was 0.9977–0.9992. Copolymer solutions in acetone were used as blank. Experiments were carried out in triplicate.

Solubility factors (f_s) were calculated according to the following equation:

$$f_s = S_a / S_{water} \quad (1)$$

where S_a and S_{water} are the apparent solubility of Pc9 in the different micellar systems and the intrinsic solubility of Pc9 in water–DMSO 2% (0.48 μg mL^{-1}), respectively. This DMSO concentration is usually the maximum concentration tolerated by cells in monolayers without significant cell death.

DLS. The average hydrodynamic diameter (D_h) and the size distribution of the polymeric micelles were measured by dynamic light scattering (DLS) using a Zetasizer Nano-Zs (Malvern Instruments, Worcestershire, UK) provided with a He-Ne (633 nm) laser and a digital correlator ZEN3600, at 25°C. Measurements were conducted at a scattering angle of $\theta = 173°$ to the incident beam. Samples were measured in a 10 × 10 mm quartz cuvette. Experiments were carried out without photosensitizer to prevent fluorescence interference in the DLS signals. Results are expressed as the average of at least three measurements.

TEM. The morphology of Pc9-free and Pc9-loaded micelles was characterized by means of transmission electron microscopy (TEM; Phillips EM 301 TEM apparatus operating at 65 kV). A sample drop was placed onto a grid covered with Formvar film and the excess was drawn off with a filter paper. Samples were subsequently stained with uranyl acetate solution for 30 s and finally dried in a closed container with silica gel and analyzed.

Photophysical characterization. Absorption and emission spectra were recorded at different concentrations using a 10 × 10 mm quartz cuvette (0.1–1 μM). Fluorescence spectra were monitored with a QuantaMaster Model QM-1 PTI spectrofluorometer (PhotoMed GmbH, Seefeld, Germany). All experiments were performed at room temperature. Emission spectra of Pc9 were collected at an excitation wavelength of 610 nm (Q-band) and recorded between 630 and 800 nm. Emission and absorption spectra of Pc9-loaded polymeric micelles were corrected for light scattering by subtracting the spectra of Pc9-free micelles.

Fluorescence quantum yields (Φ_F) were determined by comparison with those of tetra-*t*-butyl phthalocyaninatozinc(II) ($\Phi_F = 0.30$ in toluene; 30) as a reference at $\lambda = 610$ nm. Calculations were performed according to the following equation:

$$\Phi_F^S = \Phi_F^R \frac{I^S(1 - 10^{-A^R})}{I^R(1 - 10^{-A^S})} \left(\frac{n^S}{n^R}\right)^2 \quad (2)$$

where R and S superscripts refer to the reference and the sample respectively; I is the integrated area under the emission spectrum; A is the absorbance of solutions at the excitation wavelength and $(n^S/n^R)^2$ stands for the refractive index correction. The experiments were carried out in triplicate.

The quantum yield of singlet oxygen generation (Φ_Δ) was calculated by means of standard chemical monitor bleaching rates (31). For Φ_Δ studies in organic solvent, DPBF was used as a singlet oxygen chemical quencher. To avoid chain reactions induced by DPBF in the presence of singlet oxygen, the absorbance of DPBF was kept under 1.9. DPBF decay at 410 nm was monitored. For Φ_Δ studies in aqueous media, singlet oxygen monitor solutions of imidazole (8 mM) and *N*,*N*-diethyl-4-nitrosoaniline (40–50 μM) were air saturated and irradiated. The bleaching of nitrosoaniline was followed spectrophotometrically at 440 nm as a function of time. Polychromatic irradiation was performed using a projector lamp (Philips 7748SEHJ, 24V–250 W) and a cut-off filter at 610 nm (Schott, RG 610). A water filter was used to prevent infrared radiation. Samples of Pc9 and references 2,3,9,10,16,17,23,24-octakis(decyloxy) phthalocyaninatozinc(II) ($\Phi_\Delta = 0.70$ in THF; 16) and MB ($\Phi_\Delta = 0.56$ in water; 32) were irradiated within the same wavelength interval λ_1–λ_2, and Φ_Δ was calculated according to the following equation:

$$\Phi_\Delta^S = \Phi_\Delta^R \frac{r^S}{r^R} \frac{\int_{\lambda_1}^{\lambda_2} I_0(\lambda)(1 - 10^{-A^R(\lambda)})d\lambda}{\int_{\lambda_1}^{\lambda_2} I_0(\lambda)(1 - 10^{-A^R(\lambda)})d\lambda} \quad (3)$$

where r is the singlet oxygen photogeneration rate and the superscripts S and R stand for the sample and reference, respectively, A is the absorbance at the irradiation wavelength and $I_o(\lambda)$ is the incident spec-

Table 1. Structural properties, HLB and CMC of the different PEO-PPO block copolymers employed in the study.

Copolymer	Molecular weight* (kDa)	$N^{\dagger}_{EO}$	$N^{\dagger}_{PO}$	HLB‡	CMC[28] 25°C (%wt/vol)
T304	1.65	15.0	17.1	12–18	2.0
T904	6.70	60.9	69.3	12–18	0.5
T1107	15	238.6	77.6	18–23	0.5
T1307	18	286.4	93.1	>24	0.2–1.0

N_{EO}, mean number of EO units per PEO block; N_{PO}, number of PO units per PPO block; CMC, critical micelle concentration; PEO-PPO; poly(ethylene oxide)poly(propylene oxide). *Molecular weight of the copolymers as reported by BASF. †Data taken from reference (24). ‡HLB, hydrophilic–lipophilic balance.

Table 2. Apparent solubility (S_a) and solubility factors (f_s) of Pc9 encapsulated into different poloxamine micelles, at 25°C.

	Pc9 in micellar systems (10%)	
Copolymer	S_a (μg mL^{-1} ; ±SD)	f_s (± SD)
T304	1.87 (0.39)	3.89 (0.81)
T904	6.48 (0.51)	13.50 (1.06)
T1107	12.10 (0.98)	25.20 (2.04)
T1307	14.30 (1.05)	29.70 (2.19)

Results are the average (±SD) of three independently prepared micellar systems. The intrinsic Pc9 solubility in water–DMSO 2% is 0.48 μg mL^{-1}.

tral photon flow (mol s^{-1} nm^{-1}). When the irradiation wavelength range is narrow, the incident intensity varies smoothly with the wavelength, and the sample and the reference have overlapping spectra, I_o can be approximated by a constant value, which may be drawn out of the integrals and canceled. The experiments were carried out in triplicate.

Photostability. The photostability of Pc9 incorporated into polymeric micelles was determined by the decay of the Q-band intensity after exposure to red light (33). The fluence rate was adjusted to 20 mW cm^{-2}. Measurements were performed under air in water. Photodegradation rate constants k were calculated by the following equation:

$$\mathrm{In}\frac{A_0}{A_t} = k \cdot t \qquad (4)$$

where t, A_0 and A_t are the irradiation time, absorbance at $t = 0$ and absorbance at different times, respectively. The experiments were carried out in duplicate.

Aggregation studies of Pc9-loaded micelles. The intensity absorption ratio of the two bands corresponding to the monomer and oligomers was calculated. The higher values of the ratio indicated a disaggregated dye form (34,35). This ratio was calculated for all Pc9-loaded micelles using the λ_{max} indicated in Table 4. These values were compared with those obtained in THF, where aggregation was not observed, and with those obtained in water–DMSO 2%.

Cells and culture conditions. Human nasopharynx carcinoma KB cells (ATCC CCL-17) were maintained in Minimum Essential Medium (MEM; Gibco, Life Technologies, Argentina) containing 10% (vol/vol) fetal bovine serum (FBS; Gibco, Life Technologies), 2 mM L-glutamine, 50 U mL^{-1} penicillin, 50 μg mL^{-1} streptomycin, 1 mM sodium pyruvate and 4 mM sodium bicarbonate, in a humidified atmosphere of 5% CO_2 at 37°C.

Dark cytotoxicity and photocytotoxicity. KB cells were plated at a density of 1×10^4 cells per well in 96-well microplates and incubated overnight at 37°C until 70–80% of confluence. Then, the culture medium was replaced by MEM containing 4% (vol/vol) FBS and different concentrations of unloaded or Pc9-loaded micelles. After 24 h, cells were washed with PBS and exposed to a light dose of 2.8 J cm^{-2} and 1.17 mW cm^{-2}, with a 150 W halogen lamp equipped with a 10 mm water filter to attenuate IR irradiation and avoid heating of the cells. In addition, a cut-off filter was used to bar wavelengths shorter than 630 nm. In parallel, nonirradiated cells were used to study dark cytotoxicity. Following treatments, cells were incubated for another 24 h and cell viability was determined by MTT reduction assay (36). Briefly, 100 μg of MTT tetrazolium salt was added and incubated for 4 h at 37°C. Formazan crystals were solubilized in 0.01 M HCl in isopropyl alcohol and the absorbance (λ = 595 nm) was measured in a Biotrack II Microplate Reader (Amersham Biosciences, Sweden).

Pc9 cellular uptake and intracellular localization. KB cells grown on coverslips were incubated with or without 0.1 μM Pc9-loaded T1107 micelle in MEM-4% (vol/vol) FBS during 24 h at 37°C in the dark.

Table 3. D_h and size distribution of micellar systems in water at 25°C.

	Peak 1		Peak 2		Peak 3		
Copolymer	D_h (nm)	%	D_h (nm)	%	D_h (nm)	%	PDI (±SD)
T304	2.7 (0.05)	31.5	13.9 (0.35)	7.8	235.4 (7.36)	60.7	0.38 (0.04)
T904	4.1 (0.06)	13.5	14.6 (0.42)	61.1	188.0 (21.3)	25.4	0.19 (0.02)
T1107	4.3 (0.05)	32.1	22.6 (0.33)	29.6	240.9 (10.2)	38.3	0.41 (0.02)
T1307	4.9 (0.03)	22.1	47.6 (0.19)	48.4	405.3 (13.1)	29.5	0.34 (0.04)

PDI, Polydispersity index.

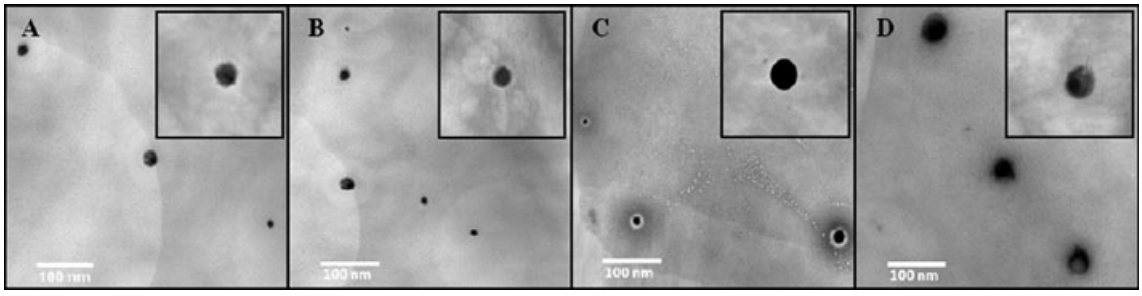

Figure 2. TEM micrographs of 10% poloxamine solutions prepared in water. Inset: TEM of Pc9-loaded micelles. T304 (A), T904 (B), T1107 (C) and T1307 (D).

After washing with PBS, cells were stained with LysoTracker Green DND-26 (75 nM, 30 min) and MitoTracker Green FM (100 nM, 45 min) as described previously (14,15). Coverslips were fixed for 10 min at room temperature with 4% (wt/vol) paraformaldehyde and cells were then examined by fluorescence. Digital images were collected in a Zeiss LSM Meta laser scanning confocal microscope (Carl Zeiss, Jena, Germany) equipped with a krypton–argon laser. Pc9 was excited at 633 nm and the emission was monitored at wavelengths higher than 650 nm. Organelles (lysosomes and mitochondria) were excited at 488 nm and green fluorescence was detected at 505–530 nm. Cell nuclei were stained with Hoechst 33258, excited at 405 nm and detected at 420–480 nm.

RESULTS AND DISCUSSION

Solubilization of Pc9 into the polymeric micelles

The first goal of the study was to explore the ability of poloxamine polymeric micelles to host Pc9 molecules within the micellar core as a strategy to enhance the water solubility of the dye. The intrinsic Pc9 solubility in water–DMSO 2% is 0.48 μg mL^{-1}. Encapsulation assays were carried out with copolymer concentrations far above the CMC (10% wt/vol) to ensure the presence of micelles and to maximize the solubilizing properties of the amphiphile (28,37,38). To comparatively evaluate the parameters that govern the solubilization in the micelles, copolymers displaying different molecular weight and hydrophilic–lipophilic balance (HLB) were used (Table 1).

In general, for similar molecular weight, more hydrophobic copolymers (lower HLB) displayed greater solubilization capacity. In addition, for similar HLB values, higher molecular weights resulted in larger cores with higher solubilizing capacity. Accordingly, T904 (MW 6.7 kDa; HLB = 12–18) showed a greater capacity than T304 (MW 1.65 kDa; HLB = 12–18; Table 2); resulting in S_a values of 1.87 and 6.48 μg mL^{-1}, respectively, representing a 3.9- and 13.5-fold solubility increase. It is worth stressing that due to a relatively small molecular weight, T304 displays an extremely low micellization tendency and solubilization capacity (28). A similar phenomenon was observed with T1107 and T1307, two highly hydrophilic poloxamines. Moreover, T1107 and T1307 were more effective than T904, showing a 25.2- and 29.7-fold solubility increase respectively. This behavior stems from the larger core generated by copolymers of greater molecular weight, independently of the HLB. In fact, T904, T1107 and T1307 contain 69.3, 77.6 and 93.1 PO units, respectively.

These results are in full agreement with previous studies (37,38) and indicate that the size of the micellar core is the predominant parameter influencing the solubilization of Pc9 (39,40).

Micellar size

The average D_h and size distribution of the micellar systems in water at 25°C were measured by DLS (Table 3). As shown in Table 3, polymeric micelles displayed several peaks at 25°C. The first peak (2.7–4.9 nm) corresponds to copolymer monomers or small micelles and the second one to polymeric micelles (13.9–47.6 nm); the greater the molecular weight of the copolymer, the greater the D_h of the Pc9-loaded micelles (Table 3). A third peak of diameter >180 nm could be attributed to partially formed aggregates that stem from the incomplete self-aggregation of PEO-PPO copolymers at 25°C (24). This behavior was specially noticeable for the low-molecular weight T304 that displays a relative high CMC (28). Then, the greater the molecular weight and the smaller the CMC (and the higher the micellization tendency), the smaller the contribution of this size population. An additional parameter that could contribute to the

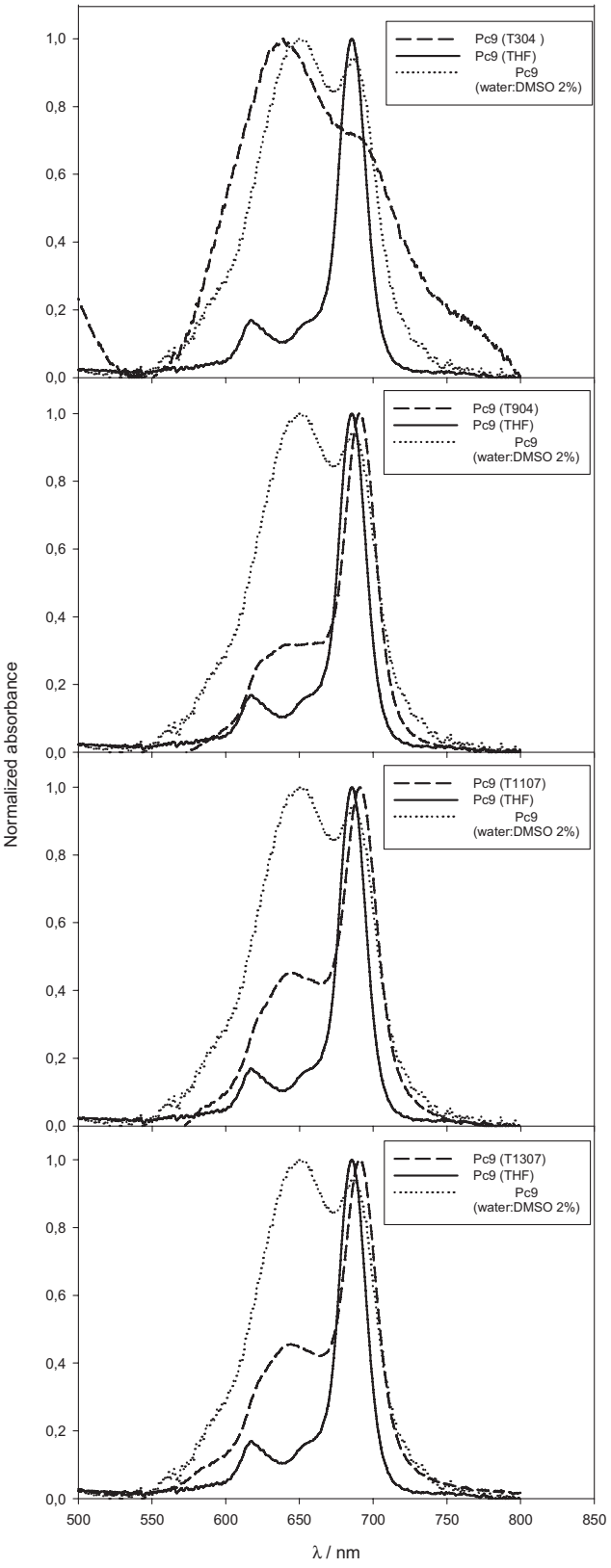

Figure 3. Absorption spectra of Pc9 (1 mM) in polymeric micelles (—), THF (–) and water–DMSO 2% (····).

Table 4. Photophysical parameters and photodegradation constants k of Pc9 in THF, water–DMSO 2% and inside polymeric micelles.

Photophysical parameters	THF	Water–DMSO 2%	T304	T904	T1107	T1307
$\lambda_{max\ absorption}$ (nm)	686	685, 650*	691, 639*	691, 640*	691, 645*	691, 646*
$\lambda_{max\ emission}$ (nm)	691	690.5	697.5	699	698.5	698.5
Φ_F[†]	0.28 ± 0.03	<0.001	0.12 ± 0.02	0.23 ± 0.01	0.20 ± 0.01	0.23 ± 0.03
Φ_Δ[‡]	0.60 ± 0.02	—[¶]	0.12 ± 0.01	0.51 ± 0.02	0.27 ± 0.02	0.35 ± 0.02
k (10^{-3} min^{-1})[§]	0.4 ± 0.05	7.82 ± 0.09	4.01 ± 0.09	5.16 ± 0.09	2.7 ± 0.06	4.52 ± 0.08
Intensity absorption rate	6.09	0.89	0.71	3.16	2.21	2.20

*Absorption corresponding to monomer and oligomer species. [†]Fluorescence quantum yield, Mean ± SD (n = 3). [‡]Singlet molecular oxygen quantum yield, Mean ± SD (n = 3). [§]Photodegradation constant, Mean ± SD (n = 3). [¶]Φ_Δ value could not be determined.

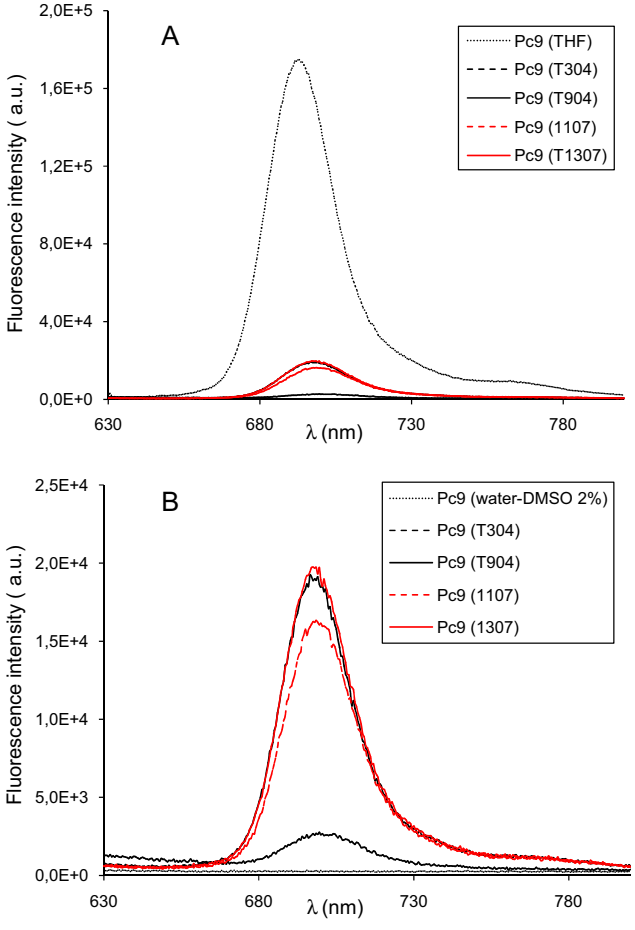

Figure 4. Emission spectra of Pc9 (1 μM) encapsulated into polymeric micelles (A and B), THF (A) and water–DMSO 2% (B). λ = 610 nm.

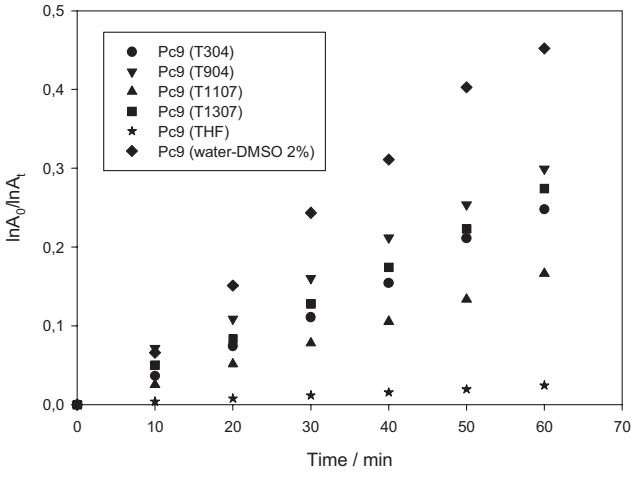

Figure 5. First-order plots for the photodegradation of Pc9 in polymeric micelles, THF and water–DMSO 2%.

generation of this size fraction is the presence of more insoluble polymer fractions (28). As intensity-weighted distributions are being plotted and the intensity is proportional to the square of the molecular weight, the larger clusters could contribute importantly to the scattered intensity and results in some overestimation of the incidence of this fraction (28,41). In any event, these larger structures remain relatively small and they are expected to disappear upon heating to 37°C due to the more complete micellization of the copolymers at higher temperature (24).

Morphology of Pc9-free and Pc9-loaded micelles

The morphology of Pc9-free and Pc9-loaded micelles was investigated by TEM. Micelles showed the characteristic spherical morphology and the coexistence of aggregates of different sizes (Fig. 2). In full agreement with the data found by DLS, an increase in the PO/PEO ratio resulted in an increase in D_h.

Photophysical characterization

Figure 3 shows the UV–Visible spectra of Pc9 (1 μM) in polymeric micelles, in THF (nonaggregating medium) and in water–DMSO 2% (aggregating medium). Pc9 in water–DMSO 2% showed a broad peak with a maximum at 650 nm, which points out aggregation. The Q-band of Pc9-loaded micelles displayed a slight broadening as well as a bathochromic shift from 686 to 691 nm in comparison with that obtained in THF. Besides, the two small vibrational bands of Pc9 in THF at 615 and 650 nm merged into one broad peak with a maximum at 639–645 nm (Table 4). These results suggest that Pc9 is present in an aggregated form in the micelle core (23,42). This effect was more marked in the T304 formulation, indicating a stronger aggregation tendency in comparison with the other systems. T304 does not micellize well and the possible formation of T304/Pc9 complexes cannot be ignored. In such complexes, Pc9 exposure to the aqueous medium is greater than in micelles, leading to greater aggregation tendency.

The fluorescence emission spectra of Pc9 (1 μM) incorporated into polymeric micelles are shown in Fig. 4 and fluorescence maxima ($\lambda_{max\ emission}$) are given in Table 4. A redshift and quenching in the fluorescence peak maximum was observed for Pc9-loaded micelles in relation to that obtained in THF (Fig. 4A), suggesting that in the micelle Pc9 is present in an aggregated form at the studied concentration. This aggregation

led to lower emission intensities of Pc9 due to self-quenching induced by interchain π–π interactions, as observed by UV–Vis spectroscopy. On the other hand, Pc9-loaded micelles presented a substantially lower aggregation tendency when compared with water–DMSO 2% (Fig. 4B, Table 4), indicating that the incorporation into polymeric micelles induced further disaggregation of Pc9. This feature would probably improve its photodynamic properties in biological media (see below).

The Φ_F value of Pc9 in THF ($\Phi_F = 0.28$) is similar to that obtained for the monomer of tetrasubstituted zinc(II) phthalocyanines (Table 4; 30). Pc9 incorporated into poloxamine micelles presented lower values of Φ_F (0.12–0.23) than those obtained in THF and higher than those obtained in water–DMSO 2%. Φ_F differences in both media could be attributed to two effects: (1) the environment contribution with a nonradiative process of electronic-to-vibrational energy and (2) the presence of aggregates (43,44). However, these values allow Pc9 to be used as photodiagnostic agent and photosensitizer in neoplasic diseases (45).

The singlet molecular oxygen quantum yield in THF was similar to those previously published (30) corresponding to Pc9 monomers at the concentrations used. The Pc9 incorporated into all micellar formulations generated singlet molecular oxygen. In addition, a decrease in the Φ_Δ values, as compared with those obtained in THF, strongly suggest that Pc9 is incorporated into the micellar core as aggregates. However, the Φ_Δ values of all micelles were higher than those obtained with other zinc(II) phthalocyanines incorporated into dimyristoyl-L-α-phosphatidylcholine (DMPC) liposomes and Tween 80® ($\Phi_\Delta < 10^{-3}$; 16), demonstrating that poloxamine micelles substantially improve the Pc9 photodynamic properties. Moreover, Pc9 incorporated into T904 showed the highest Φ_Δ value, showing that this medium induced the most efficient disaggregation of all the copolymers. In contrast, the lowest Φ_Δ was obtained for T304, indicating a significant aggregation of Pc9 in this medium. These values suggest that the HLB of the copolymer is the key parameter governing the disaggregation in the micellar core irrespective of the molecular weight and the core size. Normally, the more hydrophobic the copolymer, the greater the isolation of the encapsulated molecule from the aqueous medium (46). The opposite was true for T304, which showed a very inefficient micellization and did not encapsulate Pc9.

Photostability

The photostability of Pc9-loaded micelles was analyzed in water by measuring the decrease in the intensity of the Q-band over the time period of irradiation with red light under air (Fig. 5). The time decay of the absorbance maxima of the Q-band for Pc9 obeyed first-order kinetics. The corresponding photodegradation constants k for Pc9 are listed in Table 4. Smaller values of k indicate a higher photostability. Pc9 incorporated into polymeric micelles is more stable than that in water–DMSO 2%. The lowest k value was obtained for T1107, indicating that this was the most stable system. On the other hand, findings did not follow a trend based on the molecular features of the copolymers.

Aggregation studies of Pc9-loaded micelles

The intensity absorption rate values observed in micelles T904, T1107 and T1307 were approximately three times higher than those observed in water–DMSO 2% indicating a lower aggregation behavior for Pc9-loaded micelles. This feature could be attributed to the hydrophobic interaction between micelles and Pc9, thus decreasing the rate of aggregation. Similar aggregation values were obtained for Pc9-loaded in T304 and in water–DMSO 2%.

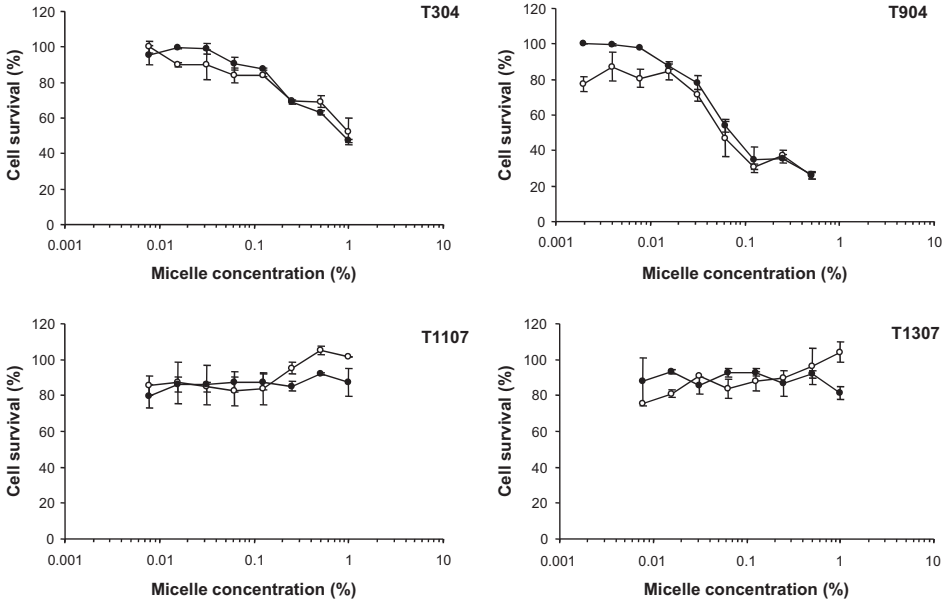

Figure 6. Effect of various micelles on KB cell viability. Different concentrations of micelles T304, T904, T1107 and T1307 were incubated with KB cells in the dark (●) or exposed to a light dose of 2.8 J cm^{-2} (○). The MTT cytotoxicity assay was carried out 24 h after treatment, as described under Materials and methods. Results are expressed as the percentage of cell growth with respect to that obtained in the absence of micelles (control) and represent the mean ± SEM of three different experiments.

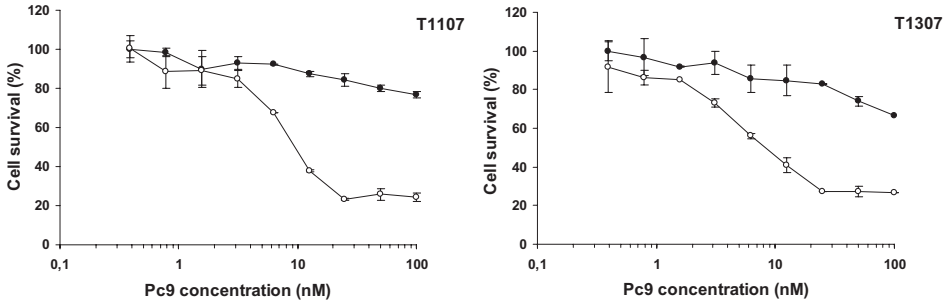

Figure 7. Effect of Pc9-loaded micelles on KB cell viability. Different concentrations of Pc9 prepared in micelles T1107 and T1307 were incubated with KB cells in the dark (●) or exposed to a light dose of 2.8 J cm^{-2} (○). Cell growth was determined by MTT assay 24 h after treatment. Results are expressed as the percentage of cell viability with respect to that obtained in the absence of Pc9 micelles (control) and represent the mean ± SEM of three different experiments.

Photobiological assays

The effect of different concentrations of Pc9-loaded micelles on KB cells was evaluated in the dark and upon exposure to a light dose of 2.8 J cm^{-2} and 1.17 mW cm^{-2}, using the MTT assay. First, the effect of empty micelles on cell viability was assessed. As shown in Fig. 6, a similar behavior was obtained for all the micelles both in the dark and in the presence of light. Cytotoxicity was observed after incubating KB cells with concentrations >0.1% of T304 micelles and 0.02% of T904 micelles, whereas T1107 and T1307 micelles showed no cytotoxic effect up to 1% concentration (Fig. 6). These values are in full agreement with previous investigations conducted with other cell lines such as Caco-2, Huh-7 and HepG-2 (47,48). As micelles T304 and T904 diminished cell growth even in the absence of light, they were not further studied.

The photocytotoxicity of Pc9-loaded micelles was examined from a maximum of Pc9 concentration of 100 nM, which corresponds to micellar concentrations of 0.10% and 0.18% for T1107 and T1307, respectively. Pc9 incorporated into T1107 and T1307 was found to be cytotoxic after irradiation, and 50% of cell proliferation (IC_{50} values) was obtained at concentrations of 10 ± 1 and 9.5 ± 0.7 nM respectively (Fig. 7). In comparison, when dose–response curves of irradiated Pc9 dissolved in 0.4% DMSO were examined (data not shown), a significantly higher IC_{50} value (0.12 ± 0.070 μM) was obtained. These findings confirm the greater PDT capacity of Pc9 when encapsulated into the polymeric micelles in comparison with the unencapsulated Pc9, owing to the lower aggregation tendency of the encapsulated form.

Intracellular localization of Pc9 incorporated into micelles

To explore whether phthalocyanine loaded into micelles is able to reach the intracellular compartment, the emission of Pc9 red fluorescence was evaluated by confocal microscopy. As shown in Fig. 8, Pc9 was mainly localized in cytoplasm after incubating KB cells for 24 h with the phthalocyanine encapsulated in T1107. When cells were incubated with fluorescent dyes for lysosomes (LysoTracker Green) and mitochondria (MitoTracker Green), Pc9 was mainly localized within cytosolic vesicles corresponding to lysosomes, as yellow fluorescence signal was visual-

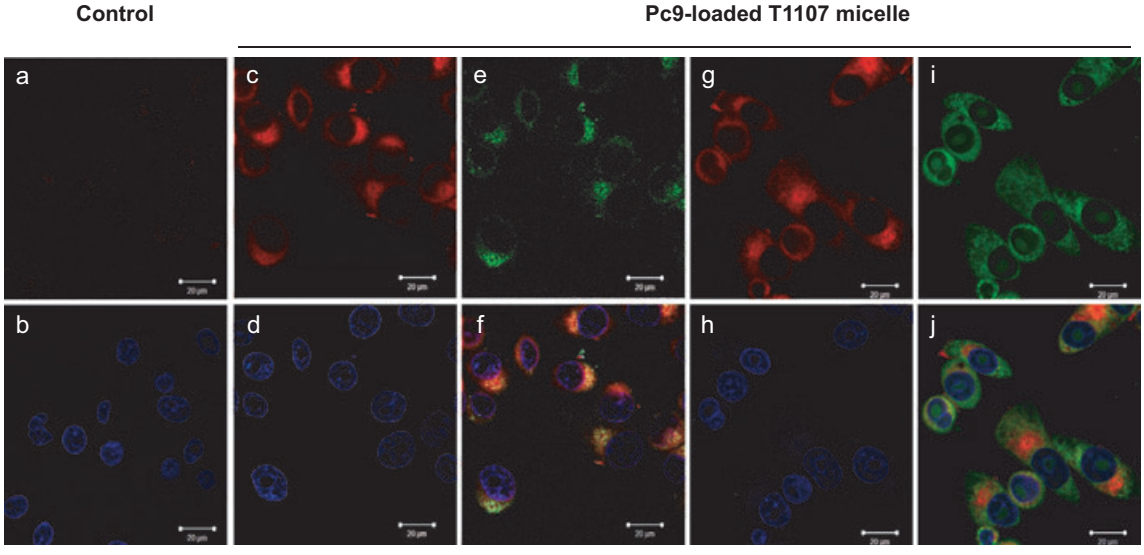

Figure 8. Cellular uptake and subcellular localization of Pc9 incorporated into micelle T1107. After incubating KB cells in the presence or absence (control) of 0.1 μM of Pc9-T1107 micelle, intracellular organelles, such as nuclei, lysosomes and mitochondria were stained with Hoechst, LysoTracker Green or MitoTracker Green respectively. Fluorescence emitted by control cells (a) or Pc9-loaded cells (c, g); cell nuclei of a, c and g (b, d and h); LysoTracker Green fluorescence (e); MitoTracker Green fluorescence (i); merge of c, d and e (f); merge of g, h and i (j). Scale bar 20 μm.

ized from the overlay of the red fluorescence from Pc9 and the LysoTracker Green probe. No colocalization was detected for Pc9 within mitochondria (Fig. 8). Similar results were obtained with Pc9-loaded T1307 micelle (data not shown).

Acknowledgements—This work was supported by grants from the University of Buenos Aires, the Consejo Nacional de Investigaciones Científicas y Técnicas (CONICET) and the Agencia Nacional de Promoción Científica y Tecnológica. Poloxamine samples were kindly provided by BASF (Verena Geiselhart). We also wish to thank the language supervision by Mrs Victoria Eusevi. J.M, L.P.R., A.S. and J.A. hold a position of Researchers at CONICET. M.C.G.V. thank CONICET for a research fellowship.

REFERENCES

1. Doughtery, T. J., C. J. Gomer, B. W. Henderson, G. Jori, D. Kessel, M. Korbelik, J. Moan and Q. Peng (1998) Photodynamic therapy. *J. Natl Cancer Inst.* **90**, 889–905.
2. Detty, M. R., S. L. Gibson and S. J. Wagner (2004) Current clinical and preclinical photosensitizers for use in photodynamic therapy. *J. Med. Chem.* **47**, 3897–3915.
3. Kato, H. (1998) Photodynamic therapy for lung cancer—A review of 19 years' experience. *J. Photochem. Photobiol. B: Biol.* **42**, 96–99.
4. Maier, A., U. Anegg, B. Fell, P. Rehak, B. Ratzenhofer, F. Tomaselli, O. Sankin, H. Pinter, F. M. Smolle-Jüttner and G. B. Friehs (2000) Hyperbaric oxygen and photodynamic therapy in the treatment of advanced carcinoma of cardia and esophagus. *Lasers Surg. Med.* **26**, 308–315.
5. Koren, H. and G. Alth (1996) Photodynamic therapy in gynaecologic cancer. *J. Photochem. Photobiol. B: Biol.* **35**, 189–191.
6. Stockert, J. C., A. Juarranz, A. Villanueva, S. Nonell, A. T. Horobin, R. W. Soltermann, N. Durantini, V. Rivarola, L. L. Colombo, J. Espada and M. Cañete (2004) Photodynamic therapy: Selective uptake of photosensitizing drugs into tumor cells. *Curr. Top. Pharmacol.* **8**, 185–217.
7. Szeimies, R. M., C. A. Morton, A. Sidoroff and L. R. Braathen (2005) Photodynamic therapy for nonmelanoma skin cancer. *Acta Derm.Venereol.* **8548**, 3–490.
8. Fabris, C., G. Valduga, G. Miotto, L. Borsetto, G. Jori, S. Garbisa and E. Reddi (2001) Photosensitization with zinc (II) phthalocyanine as a switch in the decision between apoptosis an necrosis. *Cancer Res.* **15**, 7495–7500.
9. Ali, H. and J. E. van Lier (1999) Metal complexes as photo- and radiosensitizers. *Chem. Rev.* **99**, 2379–2450.
10. Josefsen, L. B. and R. W. Boyle (2008) Photodynamic therapy: Novel third-generation photosensitizers one step closer?. *Br. J. Pharmacol.* **154**, 1–3. and references therein
11. Rumie Vittar, N. B., C. G. Prucca, C. A. Strassert, J. Awruch and V. Rivarola (2008) Cellular inactivation and antitumor efficacy of a new zinc phthalocyanine with potential use in photodynamic therapy. *Inter. J. Biochem. Cell Biol.* **40**, 2192–2205.
12. Taquet, J. P., C. Frochot, V. Manneville and M. Barberi-Heyob (2007) Phthalocyanines covantely bound to biomolecules for a targeted photodynamic therapy. *Curr. Med. Chem.* **14**, 1673–1687.
13. Strassert, C. A., G. M. Bilmes, J. Awruch and L. E. Dicelio (2008) Comparative photophysical investigation of oxygen and sulfur as covalent linkers on octaalkylamino substituted zinc(II) phthalocyanines. *Photochem. Photobiol. Sci.* **7**, 738–747.
14. Marino, J., M. C. García Vior, L. E. Dicelio, L. P. Roguin and J. Awruch (2010) Photodynamic effects of isosteric water-soluble phthalocyanines on human nasopharynx KB carcinoma cells. *Eur. J. Med. Chem.* **45**, 4129–4139.
15. Gauna, G. A., J. Marino, M. C. García Vior, L. P. Roguin and J. Awruch (2011) Synthesis and comparative photodynamic properties of two isosteric alkyl substituted zinc(II) phthalocyanines. *Eur. J. Med. Chem.* **46**, 5532–5539.
16. Rodríguez, M. E., F. Morán, A. Bonansea, M. Monetti, D. A. Fernández, C. A. Strassert, V. Rivarola, J. Awruch and L. E. Dicelio (2003) A comparative study of photophysical and phototoxic properties of octakis(decyloxy)phthalocyanintozinc (II) incorporated in an hydrophilic polymer, in liposomes and in non ionic micelles. *Photochem. Photobiol. Sci.* **2**, 988–994.
17. Konan, Y. N., R. Gurny and E. Allémann (2002) State of the art in the delivery of photosensitizers for photodynamic therapy. *J. Photochem. Photobiol. B: Biol.* **66**, 89–106.
18. Lipinski, C. (2002) Poor aqueous solubility: An industry wide problem in drug delivery. *Am. Pharm. Rev.* **5**, 82–85.
19. Rodriguez, M. E., D. A. Fernández, J. Awruch, S. E. Braslavsky and L. E. Dicelio (2006) Effect of aggregation of a cationic phthalocyanine in micelles and in the presence of human serum albumin. *J. Porphyrin Phthalocyanines* **10**, 33–42.
20. Torchilin, V. P. (2006) Multifunctional nanocarriers. *Adv. Drug Deliv. Rev.* **58**, 1532–1555.
21. Master, A. M., M. E. Rodriguez, M. E. Kenney, N. L. Oleinick and A. Sen Gupta (2010) Delivery of the photosensitizer Pc 4 in PEG-PCL micelles for *in vitro* PDT studies. *J. Pharm. Sci.* **99**, 2386–2389.
22. García Vior, M. C., E. Monteagudo, L. E. Dicelio and J. Awruch (2011) A comparative study of a novel lipophilic phthalocyanine incorporated into nanoemulsion formulations: Photophysics, size, solubility and thermodynamic stability. *Dyes Pigm.* **91**, 208–214.
23. Rijcken, C. J. F., J.-W. Hofman, F. van Zeeland, W. E. Hennink and C. F. van Nostrum (2007) Photosensitiser-loaded biodegradable polymeric micelles: Preparation, characterization and *in vitro* PDT efficacy. *J. Controlled Release* **124**, 144–153.
24. Chiappetta, D. A. and A. Sosnik (2007) Poly(ethylene oxide)-poly (propylene oxide) block copolymer micelles as drug delivery agents: Improved hydrosolubility, stability and bioavailability of drugs. *Eur. J. Pharm. Biopharm.* **66**, 303–317.
25. Sosnik, A., A. M. Carcaboso and D. A. Chiappetta (2008) Polymeric nanocarriers: New endeavors for the optimization of the technological aspects of drugs. *Recent Pat. Biomed. Eng.* **1**, 43–59.
26. Strickley, R. G. (2004) Solubilizing excipients in oral and injectable formulations. *Pharm. Res.* **21**, 201–230.
27. Van Zuylen, L., J. Verweij and A. Sparreboom (2001) Role for formulation vehicles in taxane pharmacology. *Invest. New Drugs* **19**, 125–141.
28. Gonzalez-López, J., C. Alvarez-Lorenzo, P. Taboada, A. Sosnik, I. Sandez-Macho and A. Concheiro (2008) Self-associative behavior and drug-solubilizing of poloxamine (Tetronic) block copolymers. *Langmuir* **24**, 10688–10697.
29. Alvarez-Lorenzo, C., A. Rey-Rico, J. Brea, M. I. Loza, A. Concheiro and A. Sosnik (2010) Inhibition of *P*-glycoprotein pumps by PEO-PPO amphiphiles: Branched *versus* linear derivatives. *Nanomedicine (Lond.)* **5**, 1371–1383.
30. Fernández, D. A., J. Awruch and L. E. Dicelio (1996) Photophysical and aggregation studies of *t*-butyl substituted Zn phthalocyanines. *Photochem. Photobiol.* **63**, 784–792.
31. Kraljic, I. and S. El Moshni (1978) A new method for the detection of singlet oxygen in aqueous solutions. *Photochem. Photobiol.* **28**, 577–581.
32. Wilkinson, F., W. P. Herman and A. D. (1995) Rose rate constant for the decay and reactions of the lowest electronically excited singlet state of molecular oxygen in solution. An expanded and revised compilation. *J. Phys. Chem. Ref. Data* **24**, 663–1021.
33. Schnurpfeil, G., A. K. Sobbi, W. Spillger, H. Kliesch and D. J. Wöhrle (1997) Photo- oxidative stability and its correlation with semi-empirical MO calculations of various tetraazaporphyrin derivatives in solution. *J. Porphyrins Phthalocyanines* **1**, 159–167.
34. Rodriguez, M. E., J. Awruch and L. E. Dicelio (2002) Photophysical properties of zinc(II) phthalocyaninates incorporated into liposomes. *J. Porphyrins Phthalocyanines* **6**, 122–129.
35. Alarcón, E., A. M. Edwards, M. Muñoz, A. Aspée, C. D. Borsarelli and E. A. Lissi (2009) Photophysics and photochemistry of zinc phthalocyanine/bovin serum albumin adducts. *Photochem. Photobiol. Sci.* **8**, 255–263.
36. Mossman, T. (1983) Rapid assay for cellular growth and survival: Application to proliferation and cytotoxicity assays. *J. Immunol. Methods* **65**, 55–63.
37. Chiappetta, D. A., J. Degrossi, S. Teves, M. D'Aquino, C. Bregni and A. Sosnik (2008) Triclosan-loaded poloxamine micelles for enhanced antibacterial activity against biofilm. *Eur. J. Pharm. Biopharm.* **69**, 535–545.

38. Fernandez-Tarrio, M., F. Yañez, K. Immesoete, C. Alvarez-Lorenzo and A. Concheiro (2008) Pluronic and Tetronic copolymers with polyglycolyzed oils as self-emulsifying drug delivery systems. *AAPS PharmSci. Tech.* **9**, 471–479.
39. Chiappetta, D. A., C. Hocht, C. Taira and A. Sosnik (2010) Efavirenz-loaded polymeric micelles for pediatric anti-HIV pharmacotherapy with significantly higher oral bioavailability. *Nanomedicine (Lond.)* **5**, 11–23.
40. Chiappetta, D. A., C. Hocht, C. Taira and A. Sosnik (2011) Oral pharmacokinetics of efavirenz-loaded polymeric micelles. *Biomaterials* **32**, 2379–2387.
41. Chiappetta, D. A., C. Alvarez-Lorenzo, A. Rey-Rico, P. Taboada, A. Concheiro and A. Sosnik (2010) *N*-alkylation of poloxamines modulates micellar encapsulation and release of the antiretroviral efavirenz. *Eur. J. Pharm. Biopharm.* **76**, 24–37.
42. Hirohara, S., M. Obata, S. Ogata, K. Kajiwara, C. Ohtsuki, M. Tanihara and S. Yano (2006) Sugar-dependent aggregation of glycoconjugated chlorins and its effect of photocytotoxicity in HeLa cells. *J. Photochem. Photobiol. B: Biol.* **84**, 56–63.
43. Minnes, R., H. Weitman, Y. You, M. R. Detty and B. Ehrenberg (2008) Dithiaporphyrin derivatives as photosensitizers in membranes and cells. *J. Phys. Chem. B* **112**, 3268–3276.
44. Diz, V. E., G. A. Gauna, C. A. Strassert, J. Awruch and L. E. Dicelio (2010) Photophysical properties of microencapsulated photosensitizer. *J. Porphyrins Phthalocyanines* **14**, 278–283.
45. Foote, C. S. (1991) Definition of type I and type II photosensitized oxidation. *Photochem. Photobiol.* **54**, 659–664.
46. Chiappetta, D. A., G. Facorro, E. Rubin de Celis and A. Sosnik (2011) Synergistic encapsulation of the anti-HIV agent efavirenz within poly(ethylene oxide)-poly(propylene oxide) mixed polymeric micelles. *Nanomedicine* **7**, 624–637.
47. 47.Alvarez-Lorenzo, C., A. Rey-Rico, A. Sosnik, P. Taboada and A. Concheiro (2010) Poloxamine-based nanomaterials for drug delivery. *Front. Biosci. (Elite Ed.)* **1**, 424–440.
48. Cuestas, M. L., A. Sosnik and V. L. Mathet (2011) Poloxamines display a multiple inhibitory activity of ATP-binding cassette (ABC) transporters in cancer cell lines. *Mol. Pharm.* **8**, 1152–1164.